Proceedings of
11th European Conference on Turbomachinery Fluid dynamics & Thermodynamics
ETC11, March 23-27, 2015, Madrid, Spain

EXPERIMENTAL INVESTIGATION OF FLOW WITHIN A ROTOR STATOR CAVITY

M. Micio[1] *- D. Massini*[2] *- B. Facchini*[2] *- F. Bavassano*[3] *- M. Mantero*[3]

[1] Ergon Research s.r.l.
via Panciatichi 92, 50127 Florence, Italy
mirko.micio@ergonresearch.it
[2] Industrial Engineering Department, University of Florence
via Santa Marta, 3 - 50139, Florence, Italy
[3] Ansaldo Energia
via N. Lorenzi 8, 16152 Genoa, Italy

ABSTRACT

Reliable design of secondary air system is one of the main tasks in order to ensure safety, unfailing and performance of gas turbine engines. To meet the increasing demands of gas turbines design, improved tools in prediction of the secondary air system behaviour over a wide range of operating conditions are needed. The state of the art of the fluid solver tools used to predict the flow path inside cavities is generally based on codes with correlative approaches, in order to reduce calculation times and computational resources.

To improve the prediction capabilities of a simple one-dimensional model based on correlations, the authors performed an experimental investigation on a novel test rig composed by a rotating disc facing a flat stator. Imposing several working conditions it was possible to investigate a wide range of flow regime inside the rotor-stator cavity. Rotational velocity was varied in order to gain a rotational Reynolds number up to $1.2 \cdot 10^6$, different sealing mass flows were injected within the cavity reaching a maximum turbulent flow parameter of 0.2.

Analysis of swirl development was performed by means of radial distribution of static and total pressure probes, a torque-meter was used to evaluate the frictional momentum exerted by the rotor on the fluid.

In this paper, the comparisons between experimental data and published correlations are shown to validate the experimental procedure and the postprocessing. This rig will be used for future investigation on flow field using PIV technique and heat transfer analysis on the stator using TLC with steady state tests.

NOMENCLATURE

a	Speed of sound	$[\frac{m}{s}]$
b	Outer radius of the disc	$[m]$
C_M	Moment coefficient for one side of the disc	$[-]$
C_p	Non-dimensional pressure $\frac{(P-P_{max})}{\frac{1}{2}\rho v^2}$	$[-]$
C_w	Non-dimensional mass flow rate	$[-]$
G	Gap ratio	$[-]$
$\dot{m}$	Total mass flow rate	$[\frac{kg}{s}]$
$\dot{m}_0$	Rotor mass flow rate	$[\frac{kg}{s}]$
$\dot{m}_s$	Stator mass flow rate	$[\frac{kg}{s}]$
M	Momentum on one side of the disc	$[Nm]$
M_{fd}	Momentum in free disc case	$[Nm]$
M_{rs}	Momentum in rotor-stator case	$[Nm]$
M_{off}	Bearings frictional moment	$[Nm]$
r	Radial coordinate	$[m]$
r_i	Inlet annulus radius	$[m]$
R	Universal gas constant	$[\frac{J}{kgK}]$
Re	Reynolds number	$[-]$
Re_ϕ	Rotational Reynolds number	$[-]$
Re_s	Gap Reynolds number	$[-]$
s	Axial gap between rotor and stator	$[m]$
T	Temperature	$[K]$
V_ϕ	Tangential flow velocity	$[\frac{m}{s}]$
V_t	Absolute flow velocity	$[\frac{m}{s}]$
V_r	Radial flow velocity	$[\frac{m}{s}]$
β	Core swirl ratio	$[-]$
λ_t	Turbulent flow parameter	$[-]$
μ	Dynamic viscosity	$[Pas]$
ρ	Density	$[\frac{kg}{m^3}]$
ω	Angular speed of fluid outside boundary layer	$[\frac{rad}{s}]$
Ω	Angular speed of rotor	$[\frac{rad}{s}]$

INTRODUCTION

The gas turbine Secondary Air System (SAS) provides cooling and/or sealing air to various critical parts such as turbine vanes and blades, combustion chamber, disks, internal cavities and bearing chambers, also taking into account the leakage losses. A reliable assesment of pressure in the mentioned cavities is also important for the evaluation of the net axial load acting on the thrust bearings. In design phase it is necessary to know the pressure loss in every branch of the system; however it is impossible to simulate the entire geometry using a complete CFD approach given the high number of components and their complexity. Therefore every part is studied singularly in order to obtain correlations used to improve predictions based on simplified approach requiring very poor computational resources and few calculation time.

An important part of the secondary air system is the rotor-stator cavity in which cooling air is injected in order to seal the gap between the rotor and the stator avoiding hot gas ingestion from the mainstream. The main task of designing this component is to reduce the cooling air mass flow rate assuring the gap sealed.

At designers' disposal, several relations able to predict pressure losses and gas ingestion phe-

nomena in rotor-stator systems are available since late '50s starting from the analysis of the flow structures in rotating disk systems. Batchelor (1951) proposed a non-viscous core in the solid body rotation, confined between the two boundary layers which develop on the disks. Stewartson (1953) found that the tangential velocity of the fluid can be zero everywhere apart from the rotor boundary layer. Daily and Nece (1960) before and then Daily et al. (1964), correlated their results by a direct relation between swirl ratio and turbulent flow parameter. A pioneer work in the study of flow behaviour on a rotating disk was presented by Owen and Rogers (1989), who solved this controversy reporting that at lower radii a Stewartson flow type is present (named source region) while when the fluid pumped by the rotor is greater than the injected flow, the Batchelor model onsets (named core region). The model which sets in depends therefore on the mass flow through the rotor boundary layer and the superposed one. Solving the linear Ekman-layer equation for the case of a rotor-stator system with a superimposed radial outflow of fluid, he showed that the turbulent flow parameter λ_t allows to determine the radius where the Batchelor flow type sets as reported by Owen (1989).

Poncet et al. (2005b) performed experimental and numerical investigations on transition between Stewartson and Batchelor type of flows and a new correlation to calculate the swirl ratio based on the turbulent flow parameter. A similar analysis done by Poncet et al. (2005a) was focused on stator rotor cavities with centripetal throughflow.

Innocenti et al. (2008) showed a comparison between published correlations and CFD results which highlights some discrepancies in terms of mass flow pumped within the rotor boundary layer and the swirl ratio distribution. Da Soghe et al. (2009) proposed a new correlation between the swirl number and the local turbulent flow parameter. Da Soghe et al. (2010) defined a new friction coefficients correlation which allows the calculation of the tangential velocity of the core solving the angular momentum balance. Finally Da Soghe et al. (2011) provided a correction of theoretical equation to allow a better evaluation of transition between Stewartson and Batchelor flow type.

Long et al. (2012) and Sayma et al. (2013) published both experimental and numerical analysis on the effects of bolts on the rotor disc. Finally Eastwood et al. (2012) reported their experimental investigation on the problem of ingestion in engine-like conditions.

To deepen the prediction capabilities of the rotor-cavity correlations, available in the technical literature and typically implemented in the SAS design tools, a new rotating facility for detailed measurements has been designed and commissioned at the University of Florence.

In a real rotor-stator system the hot gas ingestion can be due to the radial gradient of pressure created by the rotating air inside the wheel-space Owen (2010b) and/or due to the unsteady nonaxisymmetric variation of pressure in the annulus created by the presence of vanes and blades Owen (2010a).

The aim of this paper is to compare published correlations with experimental results obtained using a test rig designed and built in Florence University. The test rig is composed by a rotating disc facing a flat stator; the maximum rotational velocity exerted during tests was $800[RPM]$, that was the upper limit for the test rig considering the high diameter of the rotor. An annulus close to the rotating axis allows to inject the superimposed mass flow rate that can be varied using a centrifugal blower up to $150[g/s]$. Static pressure taps and total pressure Kiel probes were used to measure the pressure distribution and tangential velocity along the cavity. Moreover a torque meter was used to acquire the frictional moment exerted on the rotor.

MAIN PARAMETERS DEFINITION

In order to generalize the results discussed in this paper, it is useful to define the main nondimensional groups used in literature for stator rotor cavities.

The main parameter related to a rotating disc is the tangential Reynolds number defined as:

$$Re_\phi = \frac{\rho \Omega b^2}{\mu} \tag{1}$$

When a superposed flow is present, the nondimensional flow rate is expressed as:

$$C_w = \frac{\dot{m}}{\mu b} \tag{2}$$

The flow structure in a stator rotor cavity with superposed flow is characterized by means the combination of the previous two:

$$\lambda_t = C_w Re_\phi^{-4/5} \tag{3}$$

For example, the minimum value of mass flow necessary to prevent ingress in a unshrouded stator rotor cavity can be calculated using this parameter (the solution of the boundary layer equations provides $\lambda_t = 0.219$, see Owen and Rogers (1989)). In order to calculate the flow parameters distribution along the cavity the above global nondimensional parameter can be corrected to local values using the nondimensional ratio $x = r/b$:

- local Reynolds number:
$$Re_\phi x^2 \tag{4}$$
- local nondimensional flow rate:
$$C_w x^{-1} \tag{5}$$
- local turbulent flow parameter:
$$\lambda_t x^{-13/5} \tag{6}$$

The last nondimensional parameter is related to the tangential velocity of the core respect to that of the rotor disc, called swirl ratio and defined as:

$$\beta = \frac{\omega}{\Omega} \tag{7}$$

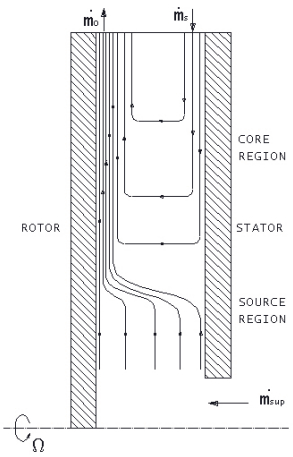

Figure 1: Flow in a stator-rotor cavity with swirl ratio lower than 1.

Solving the boundary layer equations it is clear that in presence of a rotating core the flow near the stator must be inward. Whereas, in the rotor boundary layer is outward if the swirl ratio is lower than 1, otherwise inward as demonstrated by Owen and Rogers (1989).

This implies that if the cavity is unshrouded (like in this case) and the rotor pumped mass flow rate is higher than the sealing flow injected into the cavity, for the mass continuity an ingestion from the ambient occurs through the stator boundary layer as depicted in Figure 1.

The static pressure variation in case of stator rotor cavity with superposed flow can be calculated solving the linear momentum conservation in the radial direction. To solve this equation the swirl ratio for each position must be evaluated.

Daily et al. (1964) proposed an empirical correlation to calculate the swirl ratio reduction due to the injection respect the case with no superposed flow (where $\beta = \beta^* = 0.426$) based on their experimental and numerical results:

$$\frac{\beta}{\beta^*} = \left(1 + 12.74 \frac{\lambda_t}{x^{\frac{13}{5}}}\right)^{-1} \tag{8}$$

A direct relation between the swirl ratio and the local turbulent flow parameter ($\lambda_t x^{-13/5}$) was demonstrated by Owen (1989) solving the boundary layer equations for stator rotor cavity with superposed flow. For this reason Da Soghe et al. (2009) suggested a new empirical correlation using a more extended database obtained from numerical simulation with $\lambda_t x^{-13/5}$ up to 0.4 as shown in Figure2 :

$$\frac{\beta}{\beta^*} = (1 + 7.55 \frac{\lambda_t}{x^{\frac{13}{5}}} - 13.52 (\frac{\lambda_t}{x^{\frac{13}{5}}})^2 + 188.56 (\frac{\lambda_t}{x^{\frac{13}{5}}})^3)^{-1} \tag{9}$$

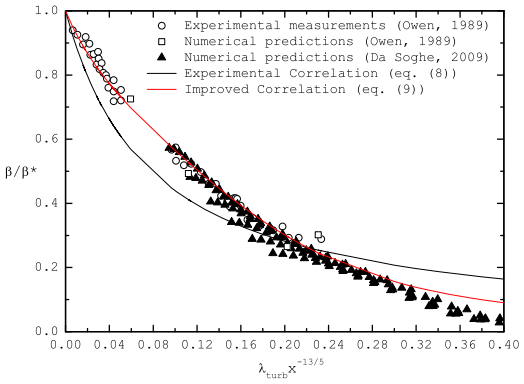

Figure 2: Variation of $\frac{\beta}{\beta^*}$ with local turbulent flow parameter $\lambda_t x^{-13/5}$. Comparison between experimental correlation (eq. 8) and improved correlation (eq. 9)

Finally, to compare the frictional torque on the rotor measured during tests with published correlation, equation 10 was used

$$C_M = \frac{M}{\frac{1}{2}\rho\Omega^2 b^5} = \frac{49\pi}{4140} |1 - \beta|^{\frac{8}{5}} (23 + 37\beta) \alpha\gamma Re_\phi^{-\frac{1}{5}} \tag{10}$$

Further details regarding the dimensionless parameter or the boundary layer solutions here presented have been published by Owen and Rogers (1989) and Owen (1989).

EXPERIMENTAL FACILITY AND PROCEDURE

In Figure 3 the test rig is showed. It is composed by a $0.962[m]$ diameter aluminum rotating disc facing a smooth stator equipped with the measurement instrumentation. The cavity clearance is $0.012[m]$ and the superposed flow is injected through an annulus close to the rotating axis and with an external diameter of $0.2[m]$. A $7.5[kW]$ WEG electric motor allows to move the rotor, it can reach a rotational speed of $1500[RPM]$.

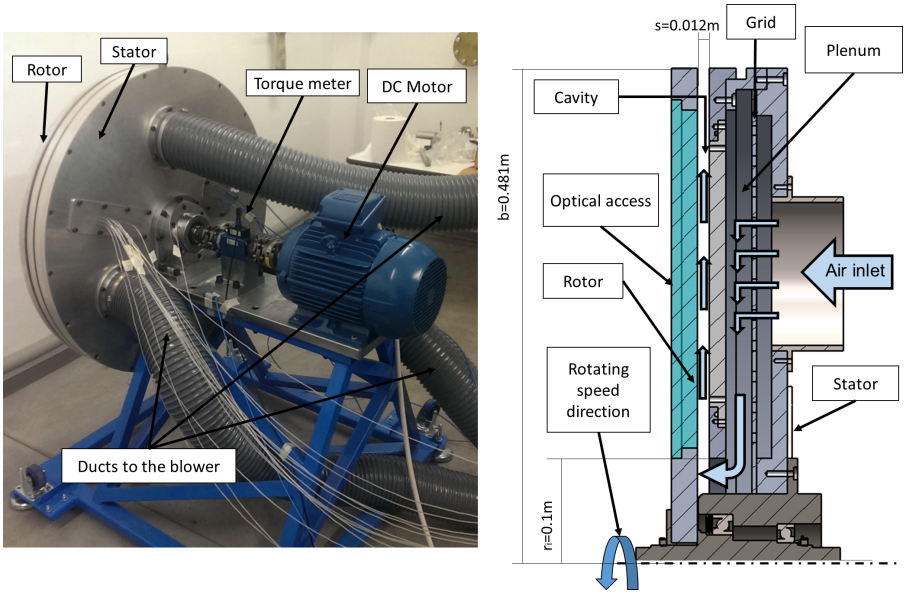

Figure 3: Test Rig

A centrifugal blower connected to the stator provides the superimposed mass flow rate up to $2.5[kg/s]$ and a $2500[Pa]$ head.

The superimposed mass flow rate is injected inside the cavity by the stator which houses the plenum and a grid to assure a good circumferential mass flow distribution entering the cavity; a section is visible in Figure 3. The stator is connected to the blower by three flexible ducts.

The Rotational Reynolds number Re_ϕ was varied up to $1.2 \cdot 10^6$ and superposed flow was adjusted to reach turbulent flow parameter λ_t up to 0.25.

The stator, see Figure 4, is equipped with 12 static pressure taps and 3 total pressure Kiel probes assuring dynamic pressure recovering for range of $\pm 40°$ for both yaw and pitch angle. The ambient temperature was measured and the flow entering the cavity was supposed at the same temperature.

Static and total pressures are measured using a pressure scanner Scanivalve DSA 3217, with temperature compensated piezoresistive relative pressure sensors, with 16 channels, uncertainty $0.1[\%]$ of the full scale that is $6900[Pa]$.

T type thermocouples with $0.5[°C]$ are used for temperature measurements, Agilent 34970A is used for the thermocouple acquisition.

For the frictional torque evaluation the Interface USB T25 Torque Sensor, with uncertainty of $\pm 0.1[\%]$ of the full scale $50[Nm]$, was used. A characterization of the frictional torque due to the transmission system was necessary.

The superimposed mass flow, at atmospheric pressure and ambient temperature, is metered through a calibrated nozzle.

The absolute velocity is calculated as difference between total and static pressure in correspondence of the Kiel probes. The tangential component of velocity (and thus the swirl ratio) is then derived as:

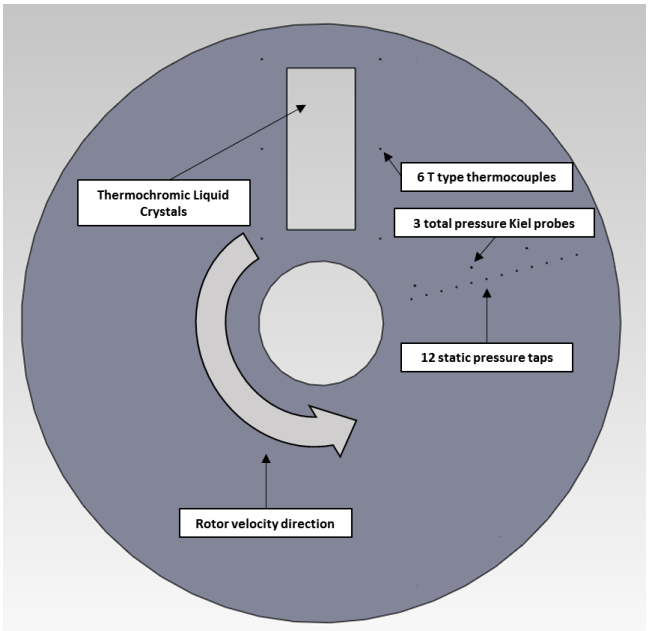

Figure 4: Stator equipped for measurement probes

$$V_\phi = \sqrt{V_t^2 - V_r^2} \tag{11}$$

$$\beta = \frac{V_\phi}{\Omega r} \tag{12}$$

being the radial component known from the measured superposed flow. In the core region the radial velocity is neglected.

EXPERIMENTAL RESULTS

Two main experimental campaigns were carried out in order to compare published correlations with experimental results. The first one concerns the tangential velocity of the core when Batchelor flow type sets in. The latter was done to verify the work extracted from the rotor by the fluid within the cavity.

Before starting with tests, a characterization of the torque losses related to the transmission system was carried out. Thus the torque was measured with both stator and rotor disks unmounted for all rotating speed that will be investigated. In order to take into account of torque variation with bearings working temperature, also the temperature of bearing casing was monitored obtaining a quadratic relation, as in equation:

$$M_{loss} = aT^2 + bT + c \tag{13}$$

The three coefficients a, b, c have been computed and collected in a data set for each rotating speed.

Free disk

First of all, frictional torque was measured in *free disc* configuration; this means that only the rotor was mounted and the torque acquired.

The goal of this first test was to compare the frictional torque evolution for different rotational speed with predicted values by equation 10. In this case the swirl ratio is equal to 0 everywhere be-

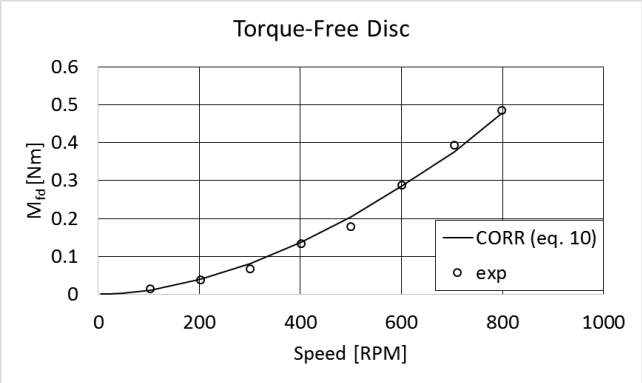

Figure 5: Free Disc-Torque vs rotating speed

cause the absence of a stator prevents the presence of the Batchelor flow type. In Figure 5, correlation and experimental results are compared showing a very good agreement.

Rotor-Stator System

In this section the frictional torque measured in case of stator rotor disk with different superposed mass flow rate are presented. Two different rotational speed were tested (500 and 700 [RPM]) which correspond to Re_ϕ equal to $7.7 \cdot 10^5$ and $1.1 \cdot 10^6$ respectively.

In order to explain the effects of sealing flow injection, results showed in Figure 6 are plotted as difference with respect to the *free disc* configuration. In fact, for high values of superposed flow, the rotating core is pushed at higher radius increasing the radial extension with a Stewartson flow type, similar to the *free disc* case. Reducing the mass flow injected into the cavity the Batchelor flow type region (where the relative velocity between fluid and rotor is lower) increases reducing the frictional torque.

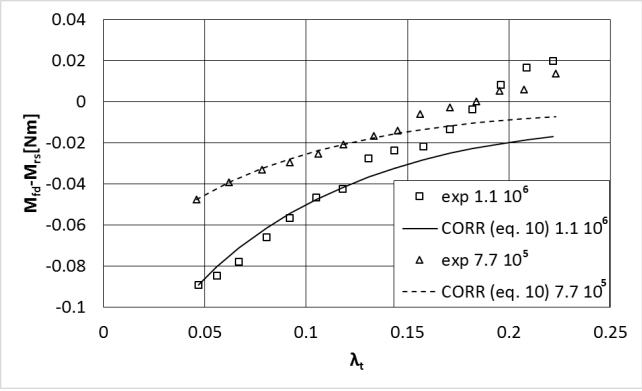

Figure 6: $M_{rs} - M_{fd}$ vs λ_t-Test for $Re_\phi = 7.7 \cdot 10^5$ and $1.1 \cdot 10^6$

This figure clearly shows that for $Re_\phi = 1.1 \cdot 10^6$ the torque variation is greater than for $Re_\phi = 7.7 \cdot 10^5$ according with correlation. In order to generalize these results, the same comparison is presented in Figure 7 where the $C_M Re^{1/5}$ are plotted instead of the torque. In this case, experimental values collapse in a curve showing a good agreement with correlation for $\lambda_t < 0.15$. Whereas, increasing the λ_t parameter, the measured values are higher than predicted ones and even greater than asymptotic value of the *free disc*. This result can be explained reminding that the superposed flow is injected in the cavity axially. This flow, impinging on the rotating disc, extracts work from the rotor resulting in a increase of frictional torque.

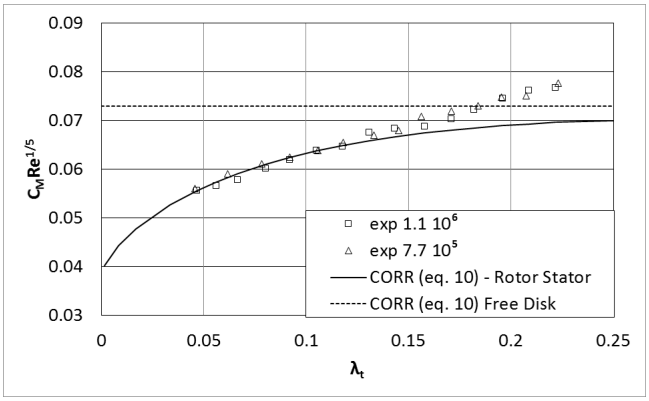

Figure 7: $C_M Re^{1/5}$ vs λ_t-Test for $Re_\phi = 7.7 \cdot 10^5$ and $1.1 \cdot 10^6$

Swirl Coefficient

In this section, the swirl ratio β obtained in correspondence of the Kiel probe (as explained in the previous section) is compared with correlations.

In Figure 8 the dashed and solid lines represent Daily et al. (1964) correlation (equation 8) and Da Soghe et al. (2009) correlation (equation 9) respectively, while the circles are experimental results. Experimental data collapse in a curve when the swirl ratio is high while becomes more dispersed when β/β^* is lower than 0.3. This fact can be explained by the fact that this swirl values correspond to very low values of tangential velocity. Being the tests performed at ambient conditions, the dynamic pressure associated to the tangential velocity assumes values close to the uncertainty of the instrumentation. For this reason the results presented in Figure 8 can be considered suitable only for high $\frac{\beta}{\beta^*}$. For this reason, swirl measurements will be planned as future works using PIV measurements to have accurate values in the whole range.

This figure shows that Daily et al. (1964) correlation (equation 8) seems to be more accurate in predicting the core swirl ratio with an higher accuracy in the whole investigated range.

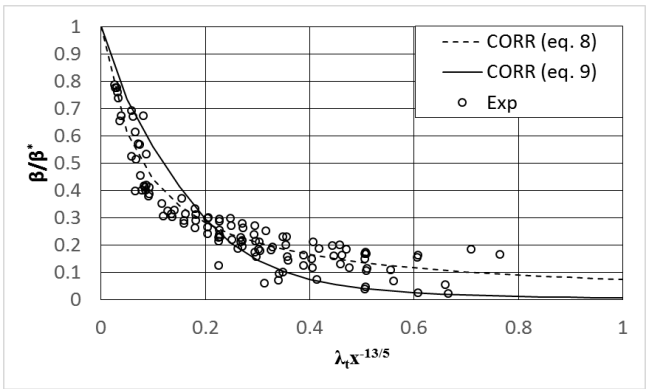

Figure 8: $\frac{\beta}{\beta^*} versus \lambda_t x^{-13/5}$

Pressure Distribution

In this section the static pressure distributions along the radius, measured using the pressure taps in different tested conditions, are compared with the pressure distribution calculated solving the linear momentum conservation in the radial direction using the swirl obtained from Daily et al. (1964) correlation (equation 8) and Da Soghe et al. (2009) correlation (equation 9). In fact the static pressure rise is due to the reduction of radial velocity (related to the increase of the passage area moving toward the outlet) and the work done to increase the core tangential velocity. In the Stewartson flow region

the first effect is dominant with a typical convex shape of the pressure rise. Whereas, in the Batchelor flow region the pressure distribution assumes a concave shape being related to quadratic therm of linear momentum equation.

Being the total turbulent flow parameter representative of the flow field inside the cavity, the static pressure distribution has a similar shape for different rotor speeds if the superposed flow is suitably varied in order to maintain the same λ_t. This is confirmed in Figure 9, where results for two different rotating velocity range are represented varying λ_t between 0.05 and 0.2. This range is representative of different working conditions of the rotating cavity. When $\lambda_t = 0.05$ the Batchelor flow type sets in at the inner part of the cavity, with consequently higher values of core swirl number. In this case the dynamic pressure recovery is negligible and all the pressure rise is located at higher radii.

Increasing the turbulent flow parameter ($\lambda_t = 0.1$), the convex part of the pressure distribution is reduced and the dynamic pressure recovery can be observed at lower radii.

Finally, for high turbulent flow parameter ($\lambda_t = 0.2$), the whole pressure rise is due to the dynamic pressure recovery at the inner part of cavity.

All these trends are well reproduced by the used model; an higher agreement between experimental and numerical data was obtained using Daily et al. (1964) correlation (equation 8), according to the better evaluation of core swirl number. According to the higher swirl number predicted by correlation 9 the pressure rise is overestimated.

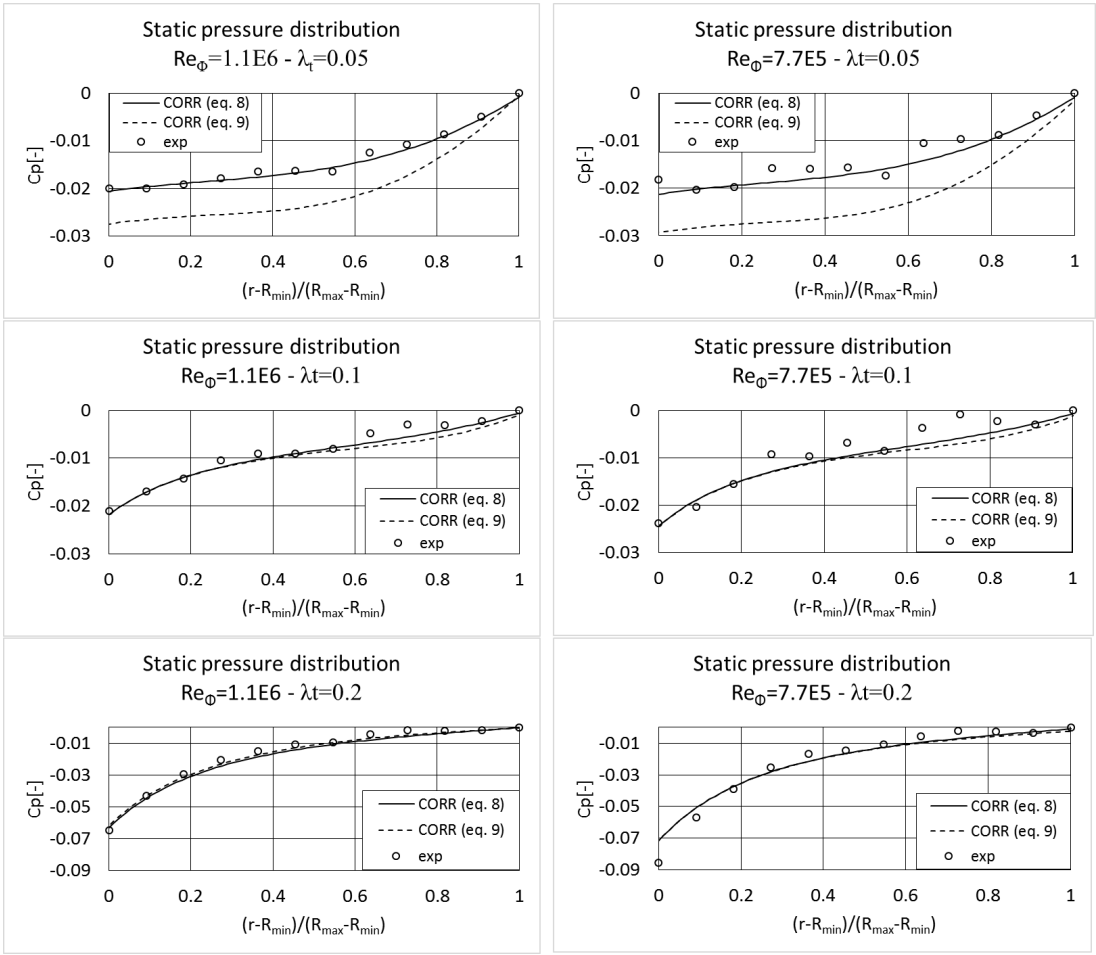

Figure 9: STATIC PRESSURE DISTRIBUTION INSIDE THE TEST RIG

CONCLUSIONS

An experimental campaign was carried out on a new rotating test rig in order to investigate the pressure and swirl distributions in a rotating cavity for different working conditions.

The maximum rotational Reyonolds number reached was $1.2 \cdot 10^6$, with a rotational velocity of $800[RPM]$. A superposed mass flow rate was injected into the cavity through an internal annulus in order to investigate different values of turbulent flow parameter.

Frictional torque measurements were performed both in free disc and rotor-stator configurations, giving results in good agreement with published correlation.

Static and total pressure probes positioned inside the cavity have been used to calculate the swirl coefficient varying the local turbulent flow parameter. These values were used to verify the accuracy of two published correlations. Daily et al. (1964) correlation is able to well predict the swirl number of the core inside the cavity resulting in a good prediction of the static pressure distribution too.

Given that the swirl evaluation from pressure probes measurements have too high uncertainty, other experimental investigations are foreseen. Particle image velocimetry (PIV) investigation is foreseen, for this reason two optical accesses are present on the rotor which allow to investigate two orthogonal planes inside the cavity. The optical accesses can also be used for heat transfer coefficient evaluation on the stator, exploiting a steady state technique: a constant heat flux can be applied through a inconel sheet covered of thermochromic liquid crystals housed by a PMMA window positioned on the stator.

The test rig can be easily updated in order to reproduce actual rotor-stator cavity geometries.

REFERENCES

G. K. Batchelor. Note on a class of solutions of the navier-stokes equations respresenting steady rotationally-symmetric flow. *Quart. J. Mech. App. Math.*, (4):29–41, 1951.

R. Da Soghe, B. Facchini, L. Innocenti, and M. Micio. Analysis of gas turbine rotating cavities by an one-dimensional model: Some improvements in a core-swirl ratio correlation. *ISABE Paper*, (ISABE-2009-1135), 2009.

R. Da Soghe, L. Innocenti, M. Micio, and B. Facchini. Analysis of gas turbine rotating cavities by an one-dimensional model: Definition of a new discs friction coefficients correlation set. *Journal of Turbomachinery*, (133(2)), 2010.

R. Da Soghe, B. Facchini, L. Innocenti, and M. Micio. Analysis of gas turbine rotating cavities: Estimation of rotor disk pumped mass flow rate. In *GT2011-46225*, pages 931–943. American Society of Mechanical Engineers, 2011.

J. W. Daily and R. E. Nece. Chamber dimension effects on induced flow and frictional resistance of enclosed rotating disks. *J. Basic Engng*, 82:217–230, 1960.

J.W. Daily, V.V. Asbedian, and W.D. Ernst. *Enclosed rotating disks with superposed throughflow: mean steady and periodic unsteady characteristics of induced flow*. Hydrodynamics Laboratory Cambridge, Mass: Report. Defense Documentation Center, Cameron Station, 1964.

D Eastwood, P R N Childs, T J Scanlon, D D Guijarro-Valencia, D D Coren, C A Long, and N R Atkins. Experimental investigation of turbine stator well rim seal, reingestion and interstage seal flows using gas concentration techniques and displacement measurements. *Journal of Engineering for Gas Turbines and Power*, 134(8):082501, January 2012.

L. Innocenti, M. Micio, R. Da Soghe, and B. Facchini. Analysis of gas turbine rotating cavities by an one-dimensional model. *ISROMAC Paper*, (12-2008-20161), 2008.

C. Long, A. L. Miles, and D. Coren. Windage measurements in a rotor stator cavity with rotor mounted protrusions and bolts. *Proceedings of ASME Turbo Expo 2012*, 2012. June 11-15, 2012, Bella Center, Copenhagen, Denmark GT2012-69385.

J. M. Owen. Prediction of ingestion through turbine rim seals-part ii: Externally induced and combined ingress. *Journal of Turbomachinery*, 133, 2010a.

J. M. Owen. Prediction of ingestion through turbine rim seals-part i: Rotationally induced ingress. *Journal of Turbomachinery*, 133, 2010b.

J M Owen and R H Rogers. *Flow and Heat Transfer in Rotating Disc Systems, Vol.1 : Rotor-Stator Systems*. Research Studies Press, Taunton, U. K., 1989.

J.M. Owen. An approximate solution for the flow between a rotating and a stationary disk. *Journal of Turbomachinery*, 111(3):323–332, 1989.

S. Poncet, M. P. Chauve, and P. Le Gal. Turbulent rotating disk flow with inward throughflow. *J. Fluid Mech.*, 522:253–262, 2005a.

S. Poncet, M. P. Chauve, and R. Schiestel. Batchelor versus stewartson flow structures in a rotor-stator cavity with throughflow. *Physics of Fluids*, 17:075110–15, 2005b.

N. Sayma, E. R. Moghaddam, and C. Long. A numerical investigation of moment coefficient and flow structure in a rotor-stator cavity with rotor mounted bolts. *Proceedings of the Institution of Mechanical Engineers, Part A: Journal of Power and Energy*, 227(3):306–327, April 2013.

K. Stewartson. On the glow between two rotating coaxial discs. *Proc. Camb. Phil. Soc*, (49):333–341, 1953.